
Incorporating NODE with Pre-trained Neural Differential Operator for Learning Dynamics

Shiqi Gong^{1,3,*}, Qi Meng², Yue Wang², Lijun Wu², Wei Chen²
Zhi-Ming Ma^{1,3}, Tie-Yan Liu²

¹University of Chinese Academy of Sciences, ²Microsoft Research Asia,

³Academy of Mathematics and Systems Science, CAS

¹gongshiqi15@mails.ucas.ac.cn, ³mazm@amt.ac.cn,

²{meq, yuwang5, lijunwu, wche, tyliu}@microsoft.com

Abstract

Learning dynamics governed by differential equations is crucial for predicting and controlling the systems in science and engineering. Neural Ordinary Differential Equation (NODE), a deep learning model integrated with differential equations, learns the dynamics directly from the samples on the trajectory and shows great promise in the scientific field. However, the training of NODE highly depends on the numerical solver, which can amplify numerical noise and be unstable, especially for ill-conditioned dynamical systems. In this paper, to reduce the reliance on the numerical solver, we propose to enhance the supervised signal in learning dynamics. Specifically, beyond learning directly from the trajectory samples, we pre-train a neural differential operator (NDO) to output an estimation of the derivatives to serve as an additional supervised signal. The NDO is pre-trained on a class of symbolic functions, and it learns the mapping between the trajectory samples of these functions to their derivatives. We provide theoretical guarantee on that the output of NDO can well approximate the ground truth derivatives by proper tuning the complexity of the library. To leverage both the trajectory signal and the estimated derivatives from NDO, we propose an algorithm called NDO-NODE, in which the loss function contains two terms: the fitness on the true trajectory samples and the fitness on the estimated derivatives that are output by the pre-trained NDO. Experiments on various of dynamics show that our proposed NDO-NODE can consistently improve the forecasting accuracy.

1 Introduction

Learning dynamics governed by differential equations is crucial for predicting and controlling the systems in science and engineering such as predicting future movements of planets in physics, protein structure prediction [30], evolution of fluid flow [27] and many other applications[23]. The recently proposed neural ordinary differential equations (Neural ODEs) [1], a deep learning model integrated with differential equations shows great promise in scientific field [11, 20, 31, 17, 2]. The continuous nature of NODEs and their differential equation structure of the hypothesis have made them particularly suitable for learning the dynamics of complex physical systems.

When we use NODE to learn the dynamics, a common setting is that we only observe the discrete trajectory samples (i.e., the coordinates of the object at a series of discrete time points) and we hope to recover its dynamics, i.e., the relation between the higher-order derivatives and its trajectory. Directly modeling the higher-order derivatives from the trajectory samples makes the training of NODE highly

*This work was done when the author was visiting Microsoft Research Asia.

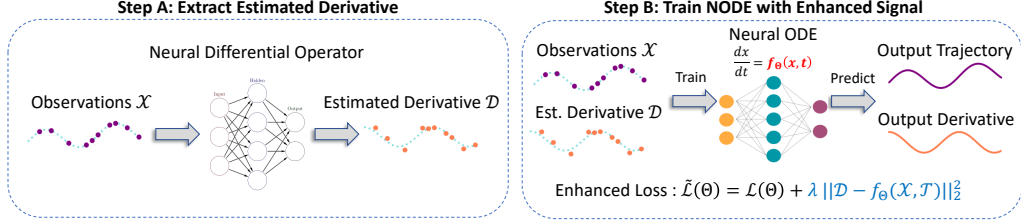


Figure 2: Illustrations of the algorithm workflow for NDO-NODE. **(A)**: extract estimated derivative from trajectory observations by a pre-trained neural differential operator. **(B)**: incorporate additional derivative signal into the training of NODE.

relies on the numerical ODE solver. Recent works [7, 31] show that the solver can amplify numerical noise and be numerically unstable, even lead to incorrect derivative signal and divergence of the training, especially for ill-conditioned dynamical systems such as stiff ODEs or chaotic systems [16, 8] as illustrated in Figure.1. There are some regularization methods designed for NODE to enforce the learned dynamics to be simple to avoid the instability such as randomizing end temporal point [8] or regularizing high-order derivative [15, 6]. These techniques can accelerate the training of NODE but their performances are still arguable when the underlying dynamics are not simple.

In this paper, to reduce the reliance on the numerical solver, we propose to incorporate common knowledge on estimating the derivatives from the trajectory samples to guide the training of NODE. The intuition is that: the differential operator is common for different functions. If we can obtain an estimation of the derivatives by learning a differential operator on a class of functions, it can directly provide guidance on learning the underlying derivatives of NODE, which is not only unaffected by the numerical instability of the ODE solver, but also help reduce the accumulated error of the solver along integrating times. Motivated by the popular pre-training techniques in machine learning [29, 5, 21, 13, 10, 28], we mine the common knowledge on estimating derivatives by pre-training a neural differential operator on a pre-designed library of symbolic functions. Specifically, the symbolic functions are composed of diverse types of functional basis such as triangle basis and polynomial basis. The NDO maps the trajectories of these functions to their derivatives. We provide theoretical guarantee on that the output of NDO can well approximate the ground truth derivatives by proper tuning the complexity of the library.

Next, when we learn an unknown dynamics, we first input the training points of the dynamics to the pre-trained neural differential operator to get the estimated derivatives. Then we use this estimation as another supervised signal in the training process of NODE by constraining the distance between estimated derivatives and the output derivatives of NODE. We name this neural ODEs algorithm as *NDO-NODE*.

We conduct experiments on various of dynamics including physical dynamics, stiff ODEs and real-world dynamics governed by differential equations to verify the effectiveness of NDO-NODE. Results show that our proposed NDO-NODE can consistently improve both the interpolation and extrapolation accuracy. Furthermore, we observe that NDO-NODE are robust to noisy and incomplete observations compared with the baselines.

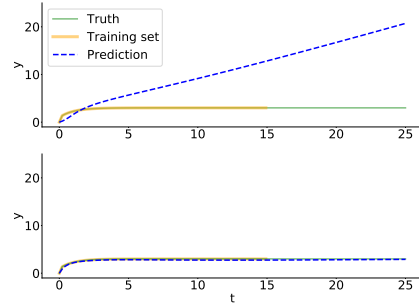


Figure 1: Vanilla NODE fails to learn this stiff ODE, while NDO-NODE does well in both fitting and forecasting. **(Top)**: Vanilla NODE. **(Bottom)**: NDO-NODE(ours).

2 Background

2.1 Neural ODEs

Neural ODEs [1] are a new family of deep neural network models that parameterize the derivative of the continuous state using a neural network. This model can be represented by ODEs:

$$\frac{dx(t)}{dt} = f_{\Theta}(x, t), \text{ s.t. } x(t_0) = x_0, \quad (1)$$

where $x(t)$ is the vector of continuous state, f_{Θ} is any kind of network with parameters Θ , and x_0 is the input state at initial time t_0 . State $x(t_i)$ can be computed by solving the initial value problem (IVP): $x(t_i) = x_0 + \int_{t_0}^{t_i} f_{\Theta}(x, t) dt = \text{ODESolve}(x_0, f_{\Theta}, t_0, t_i)$, which can be done by any numerical ODE solver.

Suppose we want to learn unknown dynamics by a sequence of trajectory observations $\mathcal{X} = (x_0, x_1, \dots, x_N)$ at times $\mathcal{T} = (t_0, t_1, \dots, t_N)$. The training process of NODE can be formulated by following optimization problem:

$$\min_{\Theta} \mathcal{L}(\mathcal{X}', \mathcal{X}) = \frac{1}{N} \sum_{i=0}^N \ell(x'_i, x_i) \quad (2)$$

$$\text{s.t. } \mathcal{X}' = (x'_0, x'_1, \dots, x'_N) = \text{ODESolve}(x_0, f_{\Theta}, t_0, \mathcal{T}), \quad (3)$$

where \mathcal{X}' is the predictions and $\ell(\cdot, \cdot)$ is a distance metric, e.g., L_1 , L_2 distance.

2.2 Related Works

Neural ODEs have recently been a popular model in scientific fields due to the continuous property. Many works apply neural ODEs to solve physical problems and forecast dynamics. Norcliffe et al. [20] extend the neural ODEs to second order and get more adaptable to classical physics governed by second order laws. Guen et al. [11] combine neural ODEs with approximate physical models to forecast the evolution of dynamical systems. Inspired by computational science and engineering, Lee and Parish [17] propose the parameterized neural ODEs that extend NODEs to have a set of input parameters, for learning multiple complex dynamics altogether.

Some previous works are proposed to better learn the dynamics by regularizing the neural ODEs. RNODE [6], which use kinetic regularization based on optimal transport, are proposed to encourage neural ODEs to prefer simpler dynamics by directly constraining the L_2 norm of first order derivative to zero. Beyond regularizing the first order derivative like kinetic regularization, Kelly et al. [15] shows that regularize the L_2 norm of the K th-order total derivatives can also help neural ODEs learn simpler dynamics. Besides regularizing the derivatives directly, Ghosh et al. [8] propose a temporal regularization that randomly sample the end time of the ODE during training, which helps find simpler dynamics and show better performance on learning stiff ODEs.

3 Algorithm: NDO-NODE

In this section, we first introduce the NDO-NODE algorithm which learns the model in Equation 1 by incorporating estimated derivatives. Then, we introduce the learning of neural differential operator to obtain the estimated derivatives.

3.1 NDO-NODE Framework

As mentioned previously, to enhance the supervised signal of NODE in learning dynamics, we propose to incorporate an estimation on the derivatives into the learning process, which directly constrains the underlying derivative of NODE. The new loss function can be expressed as

$$\tilde{\mathcal{L}} = \mathcal{L}(\mathcal{X}', \mathcal{X}) + \lambda \cdot \|\mathcal{D} - f_{\Theta}(\mathcal{X}, \mathcal{T})\|_2^2, \quad (4)$$

where $\mathcal{X}' = (x'_0, x'_1, \dots, x'_N) = \text{ODESolve}(x_0, f_{\Theta}, t_0, \mathcal{T})$ denotes the predictions of the NODE, $\mathcal{D} = (d_0, \dots, d_N)$ denotes the corresponding underlying derivatives at time points \mathcal{T} , and λ controls the strength of derivative signal. The detailed NDO-NODE algorithm is shown in Algorithm 1.

Algorithm 1 NDO-NODE

Input: Trajectory observation vector \mathcal{X} at times \mathcal{T} , query time vector $\tilde{\mathcal{T}}$, neural differential operator $\text{NDO}(\cdot)$, derivative signal strength λ

Output: Prediction vector $\tilde{\mathcal{X}}$ at times $\tilde{\mathcal{T}}$

- 1: Initialize f_Θ in neural ODEs ▷ NODEs are modeled as $\frac{dx_t}{dt} = f_\Theta(t, x_t)$
- 2: $\mathcal{D} = \text{NDO}(\mathcal{X}, \mathcal{T})$ ▷ Estimate derivative by a pre-trained NDO
- 3: **repeat**
- 4: $\mathcal{X}' = \text{ODESolve}(x_0, f_\Theta, t_0, \mathcal{T})$
- 5: $\tilde{\mathcal{L}} = \mathcal{L}(\mathcal{X}', \mathcal{X}) + \lambda \cdot \|\mathcal{D} - f_\Theta(\mathcal{X}, \mathcal{T})\|_2^2$
- 6: Update parameters Θ by $\nabla_\Theta \tilde{\mathcal{L}}$
- 7: **until** converge
- 8: **return** $\tilde{\mathcal{X}} = \text{ODESolve}(x_0, f_\Theta, t_0, \tilde{\mathcal{T}})$

Note that, although we do not know the ground truth derivative \mathcal{D} , the principle to get the derivatives for continuous functions is common. In the next section, we introduce how to pre-train a neural differential operator ($\text{NDO}(\cdot)$) to estimate the derivative \mathcal{D} from the discrete trajectory samples. As showing in Algorithm 1, we can leverage NDO to generate the estimated derivative \mathcal{D} firstly (Line 2) and then use it as an extra term into the loss function (Line 5).

3.2 Neural Differential Operator

In this section, we introduce the details to train the neural differential operator.

Algorithm 2 Learning Neural Differential Operator $\text{NDO}(\cdot)$ via Library \mathcal{Z}_{lib}

Input: Function library \mathcal{Z}_{lib}

Output: Neural differential operator $\text{NDO}(\cdot)$

Initialize network $\text{NDO}(\cdot)$.

repeat

 Randomly draw function z from \mathcal{Z}_{lib}

 Generate discretized times: $\mathcal{T}_z = (t_0, t_1, \dots, t_N)$

 Compute evaluations of function $z : \mathcal{X}_z = (z(t_0), z(t_1), \dots, z(t_N))$ and corresponding derivative $\dot{z} : \dot{\mathcal{X}}_z = (\dot{z}(t_0), \dot{z}(t_1), \dots, \dot{z}(t_N))$

$\mathcal{L} = \|\text{NDO}(\mathcal{X}_z, \mathcal{T}_z) - \dot{\mathcal{X}}_z\|_2^2$

 Update $\text{NDO}(\cdot)$ by $\nabla \mathcal{L}$

until converge

A neural differential operator $\text{NDO}(\cdot) : \mathbb{R}^N \times [0, T]^N \rightarrow \mathbb{R}^N, (\mathcal{X}, \mathcal{T}) \mapsto \mathcal{D}$, is a sequence to sequence model that project the trajectory vector \mathcal{X} at times \mathcal{T} to the corresponding estimated derivatives \mathcal{D} . Generally speaking, the neural differential operator does not depend on any specific network architecture. Networks such as fully connected neural networks or CNN can be used for trajectories with fixed time grid, while sequence model as LSTM, RNN, and transformers [26] can better cope with irregular times.

To train our NDO, we need trajectory samples $(\mathcal{X}, \mathcal{T})$ together with their true derivatives $\dot{\mathcal{X}}$ as labels. We propose to generate the training data from a synthetic function library, as it will provide us enough data without extra work like conducting physical experiments or labeling by human. However, the library becomes a key point to control the generalization ability and accuracy of the neural differential operator. In our work, we use polynomial and trigonometric functions to construct our library as they are the basis of continuous function space. Thus, the library can be written as the linear combination of the basis: $\mathcal{Z}_{lib} = \left\{ \sum_{i=0}^P [a_i \sin(it) + b_i \cos(it)] + \sum_{i=0}^Q c_i t^i \mid P, Q \in \mathbb{N}, |a_i|, |b_i|, |c_i| < C \right\}$, where a_i, b_i, c_i are coefficients of the basis, and hyperparameters P, Q and C control the complexity of our library. Given a library, our training data can be generated from the discretization values of random function sample $z \in \mathcal{Z}_{lib}$ and corresponding derivative \dot{z} . Specifically, for each one of training data, first we uniformly draw some basis and their coefficients from \mathcal{Z}_{lib} , and then

add them up to get the random function z . Its derivative \dot{z} can be computed symbolically. Then we uniformly sample time points $\mathcal{T}_z = (t_0, t_1, \dots, t_N)$ from the fixed time interval $[T_0, T_1]$ ². The sequences of evaluation $\mathcal{X}_z = (z(t_0), z(t_1), \dots, z(t_N))$ and $\dot{\mathcal{X}}_z = (\dot{z}(t_0), \dot{z}(t_1), \dots, \dot{z}(t_N))$ at times \mathcal{T}_z are the training inputs and labels, respectively. After generating training data, we minimize L_2 loss between the output of $\text{NDO}(\cdot)$ and labels $\dot{\mathcal{X}}_z$. To sum up, the training process for neural differential operator is shown in Algorithm 2. Note that, NDO is compatible for all orders of derivatives. For k -th order NDO, we just need to simply change the label to k -th order derivatives and input to $(k - 1)$ -th order derivatives.

Next, we provide the theoretical guarantee on learning the differential operator by neural networks. It has been shown that neural networks are universal approximators for non-linear operators in [3, 18]. In the next proposition, we show that the error for the learned neural differential operator $\text{NDO}(\cdot)$ and the ground truth derivative for given continuous differentiable function $g(t) : [0, 1] \rightarrow \mathbb{R}$.

Theorem 3.1. *Suppose that $\mathcal{Z}'_{lib} \subset \mathcal{Z}_{lib}$ is the training function set for NDO. The Lipschitz constant for the learned neural differential operator function is L_{NN} . For given continuous differentiable function $h(t) : [T_0, T_1] \rightarrow \mathbb{R}$, we define the distance between two functions as $\rho(h, z) = \sum_{i=1}^N |h(t_i) - z(t_i)|$, where $\{t_i\}_{i=1}^N$ equally partition the time interval $[T_0, T_1]$. $z(t) \in \mathcal{Z}'_{lib}$ is a function in the training data, $h(t)$ is an arbitrary function. The output derivative of NDO for a function is denoted using the subscription NDO. Then the error of the output derivation \dot{h}_{NDO} and the ground truth derivative \dot{h} can be upper bounded as:*

$$\rho(\dot{h}_{\text{NDO}}, \dot{h}) \leq L_{NN} \int_{T_0}^{T_1} |z(t) - h(t)| dt + \int_{T_0}^{T_1} |\dot{z}(t) - \dot{h}(t)| dt + \frac{|T_1 - T_0|^3}{12N^2} M + \rho(\dot{z}_{\text{NDO}}, \dot{z}),$$

where $M = L_{NN} \cdot \max_{t \in [T_0, T_1]} |\ddot{\epsilon}(t)| + \max_{t \in [T_0, T_1]} |\dot{\epsilon}(t)|$ with $\epsilon(t) = |z(t) - h(t)|$.

Theorem 3.1 shows that the upper bound of $\rho(\dot{h}_{\text{NDO}}, \dot{h})$ depends on three factors: the approximation error of $z(t)$ (measured by both the L_1 distance between $z(t)$ and $h(t)$ and the L_1 distance between $\dot{z}(t)$ and $\dot{h}(t)$), the smoothness of the NN model L_{NN} and the optimization error on the training data z , i.e., $\rho(\dot{z}_{\text{NDO}}, \dot{z})$. As the library becomes large, the approximation error have chances to become small but the optimization will become hard (which may cause the increase of $\rho(\dot{z}_{\text{NDO}}, \dot{z})$). Therefore, if we properly set the library that can balance the approximation ability and the optimization efficiency, it can well approximate the ground truth derivatives.

4 Experiments

We mainly consider three different scenarios of tasks to show the advantages of proposed NDO-NODE: i) physical systems, ii) stiff ODEs, and iii) real-world airplane vibration dataset.

We use these three classes of experiments to show that: i) Under different noise scales, NDO-NODE shows great promise to physical problems and has better extrapolation ability than vanilla neural ODEs, ii) the enhanced derivative signal helps neural ODEs to better learn both stiff and flat parts of the trajectory, which vanilla neural ODEs are hard to capture, and iii) NDO-NODE performs well on learning and forecasting continuous dynamics in the real world case.

In all of the following experiments, we use a LSTM model to implement $\text{NDO}(\cdot)$. We set $t_0 = 0$ and align $t_N = 1$ for the inputs to make the model simpler. Note that if $t_N \neq 1$ in input times \mathcal{T} , we can standardize \mathcal{T} by multiplying a factor $1/t_N$ to both \mathcal{T} and output derivative estimation \mathcal{D} . Moreover, we augment the input sequence as $(\mathcal{X}, \mathcal{T}, \Delta\mathcal{T}) = \{(x_i, t_i, \Delta t_i)\}_{i=0}^N$, where $\Delta t_i = t_i - t_{i-1}$, to better serve for this task. The hyperparameters of library \mathcal{Z}_{lib} are all set as $(P, Q, C) = (3, 50, 10)$. We randomly draw 10000 functions from \mathcal{Z}_{lib} and discretize them by 100 uniform random times in interval $[0, 1]$ as our training data. Please refer to Appendix for more training details.

4.1 Physical Systems

In this section, we focus on learning three widely used physical systems from their trajectories. We choose vanilla NODE [1] and RNODE [6] as our baselines, because RNODE directly constrains the

²In experiments, we fix $[T_0, T_1]$ to be $[0, 1]$

L_2 norm of derivatives f_{Θ} to zero, which is most close to our methods. We measure the accuracy by the mean square error of predictions with respect to ground truth under different noise scales.

In the following experiments, we divide the whole time range $[0, T]$ into two segments, $[0, T_1]$ and $[T_1, T_2]$. We train our model on $[0, T_1]$ and validate on both $[0, T_1]$ and $[T_1, T_2]$ for interpolation and extrapolation, respectively. For training data, we irregularly choose 100 time points from the training time range $[0, T_1]$, and generate the corresponding process states. As Norcliffe et al. [20] do, we add noises that are independently drawn from $\mathcal{N}(0, \sigma)$ to each state in training data to demonstrate the robustness of our method. For the test data, we uniformly choose 1000 time points from $[0, T_1]$ and $[T_1, T_2]$, respectively. We measure the interpolation ability by the mean square error on $[0, T_1]$ (In. MSE), and extrapolation ability by the mean square error on $[T_1, T_2]$ (Ex. MSE). For each method in our experiments, except the reusable parameters from other literature, we implement grid search on a wide range for remaining parameters and report the best numbers. Training details for these experiments can be found in Appendix.

4.1.1 Planar Spiral Systems

Linear ordinary differential systems are one of the fundamental equations and are widely used in physics [14]. We take two dimensional linear ODEs as an example, which can be written as

$$\begin{cases} \frac{dx}{dt} = ax + by \\ \frac{dy}{dt} = cx + dy \end{cases} \quad (5)$$

Chen et al. [1] studies the system with parameters $a = -0.1, b = 2, c = -2, d = -0.1$ and initial values $[x, y] = [2, 0]$, whose trajectory looks like a planar spiral coil. Following their setting, we parameterize a 2-dimensional neural ODEs with a one hidden layer network with 20 hidden units and ELU activation [4]. We set the training time range to $[0, 5]$ seconds and test extrapolation on $[5, 10]$ seconds, and Table.1 shows the results under different noise scales. NDO-NODE performs consistently better than baselines on both interpolation and extrapolation tasks, and it shows prominent advantages under low noise scale since NDO provides more accurate estimation of derivatives. Figure.3 visualizes how the learned dynamics extrapolate and the help on extrapolation from derivative signal.

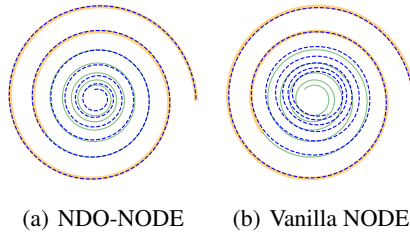


Figure 3: Ground truth (green solid), and prediction (dashed blue) of spiral systems under noise $\sigma = 0$. Training on $[0, 5]$ seconds (orange) and forecasting on $[5, 20]$ seconds (green).

Table 1: Mean squared error (MSE) (mean \pm std, $\times 10^{-2}$, over 3 runs) in planar spiral systems experiments. In. MSE (interpolation MSE) is computed on time range $[0, 5]$ seconds while Ex. MSE (extrapolation MSE) is computed on time range $[5, 10]$ seconds.

MSE	Noise	NODE	RNODE	NDO-NODE(ours)
In. MSE	0	0.026 \pm 0.014	0.040 \pm 0.019	0.012 \pm 0.004
	0.01	0.036 \pm 0.017	0.049 \pm 0.028	0.018 \pm 0.014
	0.03	0.054 \pm 0.028	0.069 \pm 0.040	0.049 \pm 0.043
	0.05	0.089 \pm 0.041	0.101 \pm 0.053	0.085 \pm 0.039
Ex.MSE	0	4.524 \pm 2.890	4.023 \pm 2.749	0.525 \pm 0.304
	0.01	5.416 \pm 3.671	4.788 \pm 3.513	0.530 \pm 0.371
	0.03	5.717 \pm 3.652	5.174 \pm 3.479	1.853 \pm 1.845
	0.05	6.332 \pm 3.902	5.729 \pm 3.671	5.347 \pm 4.193

4.1.2 Damped Harmonic Oscillator

The damped harmonic oscillator is a vibrating system whose amplitude of vibration decreases over time. It is a typical model in physics that has been widely studied [9]. From mechanics, this system

can be governed by following ordinary differential systems

$$\begin{cases} \frac{dx}{dt} = v \\ \frac{dv}{dt} = -(\omega^2 + \gamma^2)x - 2\gamma v, \end{cases} \quad (6)$$

where x, v are the position and velocity of the oscillator, and ω, γ describe the undamped angular frequency and damping coefficient. We set $\gamma = 0.1, \omega = 1$ and generate 30 random position trajectories with different initial positions and velocities, under the similar setting of Norcliffe et al. [20]. The state $[x, v]$ is modeled by a one hidden layer neural ODEs with 20 hidden units. As we only have the position trajectory, we use both 1st-order and 2nd-order NDO to extract the underlying velocity v and the acceleration $a = \frac{dv}{dt}$. We train the models on $[0, 10]$ seconds, and forecast the positions on $[10, 20]$ seconds. The results under different noise scales are listed in Table. 2. NDO-NODE provides a big improvement to both interpolation and extrapolation under low scales. When noise gets higher, NDO output inaccurate derivative estimation, which provides less information comparing to low noise scales.

Table 2: Mean squared error (MSE) (mean \pm std, $\times 10^{-3}$, over 3 runs) in damped harmonic oscillator experiments. In. MSE (interpolation MSE) is computed on time range $[0, 10]$ seconds while Ex. MSE (extrapolation MSE) is computed on time range $[10, 20]$ seconds.

	MSE	Noise	NODE	RNODE	NDO-NODE(ours)
In. MSE		0	0.522 \pm 0.195	0.206 \pm 0.087	0.100 \pm 0.031
		0.1	0.556 \pm 0.201	0.183 \pm 0.036	0.178 \pm 0.046
		0.3	0.950 \pm 0.445	0.382 \pm 0.148	0.339 \pm 0.061
		0.5	1.667 \pm 0.786	0.746 \pm 0.191	0.753 \pm 0.173
Ex.MSE		0	0.792 \pm 0.576	0.424 \pm 0.206	0.086 \pm 0.034
		0.1	0.790 \pm 0.563	0.310 \pm 0.096	0.247 \pm 0.129
		0.3	1.232 \pm 0.790	0.335 \pm 0.159	0.243 \pm 0.130
		0.5	2.052 \pm 1.195	0.466 \pm 0.233	0.463 \pm 0.223

4.1.3 Three-body Problem

The three-body problem is one of the most famous and important problems in physics and celestial mechanics, which was first proposed to model the motion of three celestial bodies [25]. By Newton’s laws of motion and Newton’s law of universal gravitation, this dynamical system is governed by

$$\frac{d^2 \mathbf{r}_i}{dt^2} = - \sum_{j \neq i} G m_j \frac{\mathbf{r}_i - \mathbf{r}_j}{|\mathbf{r}_i - \mathbf{r}_j|^3}, \quad i = 1, 2, 3, \quad (7)$$

where \mathbf{r}_i denotes the position of i th body in 3-dimensional space, m_i denotes the mass of i th body, and G stands for gravitational constant. Because this system is chaotic for most initial conditions, we integrate partial physical prior knowledge into the neural ODEs as Zhuang et al. [31] do. Specifically, we augment the input data as an 45-dimensional vector as

$$\text{Input} = \left\{ \mathbf{r}_i, \mathbf{r}_i - \mathbf{r}_j, \frac{\mathbf{r}_i - \mathbf{r}_j}{|\mathbf{r}_i - \mathbf{r}_j|^1}, \frac{\mathbf{r}_i - \mathbf{r}_j}{|\mathbf{r}_i - \mathbf{r}_j|^2}, \frac{\mathbf{r}_i - \mathbf{r}_j}{|\mathbf{r}_i - \mathbf{r}_j|^3} \right\}, j \neq i, \quad (8)$$

and the underlying derivative of neural ODEs are modeled by a one hidden layer network with 100 hidden units. To get the estimated derivations, we apply both 1st-order and 2nd-order NDO on the position of each body trajectory. We train the models on $[0, 1]$ year, and predict the position on $[1, 2]$ years. Table. 3 shows the results in terms of MSE, From Table.3, NDO-NODE shows good improvement to vanilla NODE. However, because this is a chaotic high dimensional system and we need to extract up to 2nd-order derivatives from trajectory, our library may not cover the full form of the trajectory, thus the estimated derivatives can only provide limited help for the learning. Moreover, high dimension causes the derivative space very complex, thus RNODE also performs better than vanilla NODE and has a similar performance as NDO-NODE.

4.2 Stiff ODEs

Table 3: Mean squared error (mean \pm std, $\times 10^1$, over 3 runs) in the three-body problem experiments. In. MSE (interpolation MSE) is computed on time range $[0, 1]$ year while Ex. MSE (extrapolation MSE) is computed on time range $[1, 2]$ year.

	MSE	Noise	NODE	RNODE	NDO-NODE(ours)
In. MSE		0	0.041 ± 0.011	0.039 ± 0.004	0.027 ± 0.006
		0.001	0.033 ± 0.006	0.031 ± 0.003	0.027 ± 0.003
		0.003	0.033 ± 0.001	0.030 ± 0.005	0.033 ± 0.004
		0.005	0.029 ± 0.004	0.028 ± 0.003	0.027 ± 0.004
Ex. MSE		0	0.691 ± 0.208	0.440 ± 0.198	0.434 ± 0.025
		0.001	0.994 ± 0.447	0.534 ± 0.109	0.467 ± 0.134
		0.003	1.222 ± 0.750	0.513 ± 0.103	0.489 ± 0.058
		0.005	0.985 ± 0.260	0.424 ± 0.049	0.549 ± 0.138

Stiff ODEs are widely used in modeling chemical kinetic systems [22] and biological systems [12]. This kind of ODE is a big challenge for numerical ODE solvers, that the stiffness may cause numerically unstable unless an extremely small step size is used. Thus neural ODEs need to take more time to learn stiff systems and even fail to learn in many cases [16]. To show NDO-NODE may help learn stiff ODEs, we follow the experiment in Ghosh et al. [8] and test the ODE

$$\frac{dy}{dt} = -1000y + 3000 - 2000e^{-t}, \quad (9)$$

with initial condition $y(0) = 0$. The neural ODEs are modeled by a single hidden layer network with 500 hidden units. We use the same setting for vanilla NODE and STEER as Ghosh et al. [8] do in their released code, and add derivative signal $\lambda = 0.05$ with other parameters unchanged for NDO-NODE. We train these models on time range $[0, 15]$ while forecast on range $[15, 25]$. The learned trajectories are shown in Figure.4. Vanilla NODE fails to learn this system and deviates far from the truth, while NODE with STEER and RNODE performs better but is still not accurate. NDO-NODE learns this system well and captures both stiff and flat parts of this dynamics.

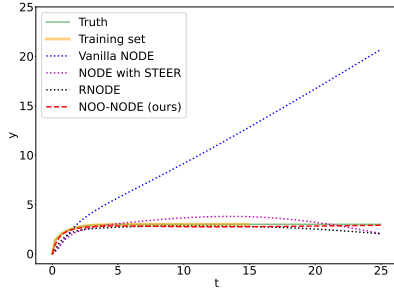


Figure 4: Results on the stiff ODE

4.3 Airplane Vibration Dataset

This dataset [19] records the acceleration signals of an aircraft based on a ground vibration test. A shaker was attached underneath the right wing to apply input signals, and the input acceleration a_1 is recorded. Acceleration a_2 is measured on the right wing next to the nonlinear interface of interest. The special structure of the airplane causes nonlinear distortions in the aircraft vibration dynamics, which brings difficulties in learning and prediction for a_2 .

Similar to [20], we test SONODE and NDO-SONODE on this dataset. The neural ODEs in both methods are parameterized as a single hidden layer neural network with 50 hidden units. We train the models on $[0, 1000]$ and forecast on $[1000, 5000]$ time units. The results are reported in Figure.5, which shows NDO-SONODE has a better performance over SONODE on this dataset.

4.4 Ablation Study

In this section, we conduct ablation studies to provide a better understanding of both signal strength λ and the effect on library complexity to the performance of the neural differential operator.

4.4.1 Signal strength λ

We take the planar spiral system task in Sec.4.1.1 as an example. We grid search λ in a wide range $[10^{-4}, 10^1]$ and keep other parameters unchanged. Results are shown in Figure 6, from which we can observe: 1) under low noise scale, the larger λ gives a better improvement especially in

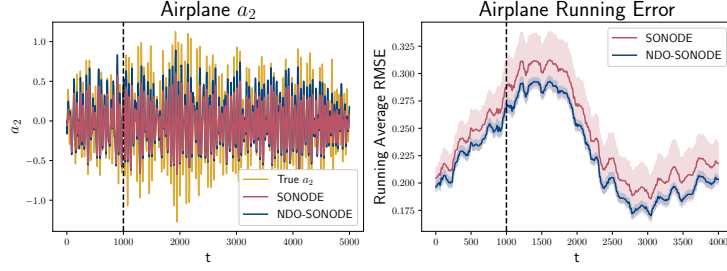


Figure 5: Results of SONODE and NDO-SONODE on airplane vibration dataset. **(Left)**: ground truth and forecasting trajectories. **(Right)**: moving averages of root mean square error (RMSE).

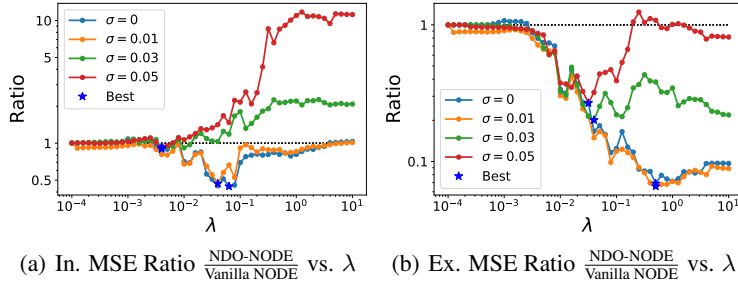


Figure 6: The interpolation and extrapolation ratio of NDO-NODE to Vanilla NODE under different noise scales σ in planar spiral system task (See Sec. 4.1.1), computed by the mean MSE over 3 runs.

extrapolation, and it also performs consistently better than baselines in interpolation; 2) under high noise scale, smaller λ should be applied, which leads to a good improvement in extrapolation while preventing the loss of interpolation; 3) among all best λ s of both interpolation and extrapolation, the more significant improvement they have, with the lower noise scales. Due to NDO outputs more accurate derivative estimations under lower noise scales, these observations are consistent with the intuition that, the enhanced derivative signal provides stronger guidance when the estimations are more accurate. Moreover, when λ is large, NODE will tend to fit the derivative estimations instead of the trajectory. Because NDO uses whole trajectory to extract the derivative estimations, it can better capture overall information and thus help extrapolation. However, the derivative estimations from NDO can not be exactly precise, thus when we use large λ , the interpolation MSE may get larger even under low noise scale, i.e., $\lambda \approx 0.1$ vs. $\lambda \approx 1$ under $\sigma = 0$ or 0.01 in this case.

4.4.2 Estimation Accuracy of NDO vs. Library Complexity

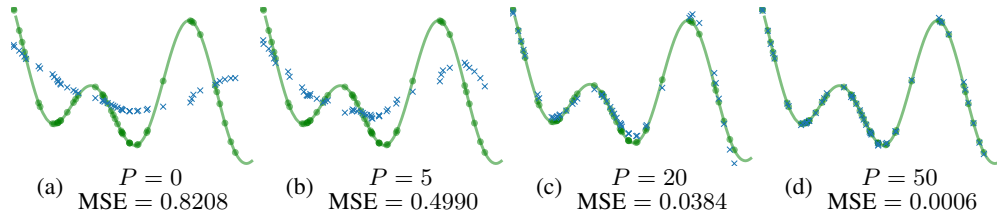


Figure 7: Estimate the derivative of $z(t) = \sin(3t)/3 + \sin(15t)/15 + \sin(30t)/30$, $t \in [0, 1]$ by NDOs, which are pre-trained by libraries with different parameter P and fixed $Q = 3$, $C = 10$. MSE between estimation (blue) and truth (green) are in the captions.

To test how the library complexity affects the accuracy of estimation, we pre-train NDOs with different libraries and use them on a specified $z(t)$ (see Figure 7). Note that $z(t)$ has 3 terms that are successively contained into the libraries with $Q = 5, 20, 50$. From Figure 7, we observe that the accuracy of estimations gets higher when more terms can be contained in the library. When the

library can not cover $z(t)$, i.e., $Q = 0, 5, 20$, NDO will fit the main parts that the library contains. When the library fully covers $z(t)$, i.e., $Q = 50$, the estimation gets very close to the ground truth derivatives, which agrees with our theoretical results.

5 Conclusion

To enhance the supervised signal in learning dynamics, we propose an algorithm called NDO-NODE, which leverage the estimated derivatives from trajectory samples, to enhance the supervised signal of the NODE training process. The estimated derivatives are obtained by a pre-trained neural differential operator. With the supervision of estimated derivatives, NDO-NODE can improve the forecasting accuracy on various dynamics and it is robust to noisy and incomplete observations. In the future, we will continue to explore how efficiently pre-train the neural differential operator for learning latent ODEs and multi-agent dynamical systems.

References

- [1] R. T. Q. Chen, Y. Rubanova, J. Bettencourt, and D. Duvenaud. Neural Ordinary Differential Equations. *arXiv:1806.07366 [cs, stat]*, 2018.
- [2] R. T. Q. Chen, B. Amos, and M. Nickel. Learning Neural Event Functions for Ordinary Differential Equations. *arXiv:2011.03902 [cs, stat]*, Nov. 2020.
- [3] T. Chen and H. Chen. Universal approximation to nonlinear operators by neural networks with arbitrary activation functions and its application to dynamical systems. *IEEE Transactions on Neural Networks*, 6(4):911–917, 1995.
- [4] D.-A. Clevert, T. Unterthiner, and S. Hochreiter. Fast and accurate deep network learning by exponential linear units (elus). *arXiv preprint arXiv:1511.07289*, 2015.
- [5] J. Devlin, M.-W. Chang, K. Lee, and K. Toutanova. Bert: Pre-training of deep bidirectional transformers for language understanding. *arXiv preprint arXiv:1810.04805*, 2018.
- [6] C. Finlay, J.-H. Jacobsen, L. Nurbekyan, and A. Oberman. How to Train Your Neural ODE: The World of Jacobian and Kinetic Regularization. In *International Conference on Machine Learning*, pages 3154–3164. PMLR, Nov. 2020.
- [7] A. Gholaminejad, K. Keutzer, and G. Birocs. Anode: Unconditionally accurate memory-efficient gradients for neural odes. In *Proceedings of the Twenty-Eighth International Joint Conference on Artificial Intelligence, IJCAI-19*, pages 730–736. International Joint Conferences on Artificial Intelligence Organization, 7 2019. doi: 10.24963/ijcai.2019/103. URL <https://doi.org/10.24963/ijcai.2019/103>.
- [8] A. Ghosh, H. Behl, E. Dupont, P. Torr, and V. Namboodiri. Steer: Simple temporal regularization for neural ode. *Advances in Neural Information Processing Systems*, 33, 2020.
- [9] H. Goldstein, C. Poole, and J. Safko. *Classical mechanics*, 2002.
- [10] P. Goyal, P. Dollár, R. Girshick, P. Noordhuis, L. Wesolowski, A. Kyrola, A. Tulloch, Y. Jia, and K. He. Accurate, large minibatch sgd: Training imagenet in 1 hour. *arXiv preprint arXiv:1706.02677*, 2017.
- [11] V. L. Guen, Y. Yin, J. Dona, I. Ayed, E. de Bézenac, N. Thome, and P. Gallinari. Augmenting Physical Models with Deep Networks for Complex Dynamics Forecasting. *arXiv:2010.04456 [cs, stat]*, Oct. 2020.
- [12] J. W. Haefner. *Modeling Biological Systems:: Principles and Applications*. Springer Science & Business Media, 2005.
- [13] K. He, R. Girshick, and P. Dollar. Rethinking imagenet pre-training. In *Proceedings of the IEEE/CVF International Conference on Computer Vision (ICCV)*, October 2019.
- [14] R. L. Herman. Herman, russell l. 2017. a first course in differential equations for scientists and engineers, Mar 2018. URL <https://www.simiode.org/resources/4452>.

- [15] J. Kelly, J. Bettencourt, M. J. Johnson, and D. Duvenaud. Learning differential equations that are easy to solve. *arXiv preprint arXiv:2007.04504*, 2020.
- [16] S. Kim, W. Ji, S. Deng, and C. Rackauckas. Stiff neural ordinary differential equations. *arXiv preprint arXiv:2103.15341*, 2021.
- [17] K. Lee and E. J. Parish. Parameterized neural ordinary differential equations: Applications to computational physics problems. *arXiv preprint arXiv:2010.14685*, 2020.
- [18] L. Lu, P. Jin, G. Pang, Z. Zhang, and G. E. Karniadakis. Learning nonlinear operators via deep-onet based on the universal approximation theorem of operators. *Nature Machine Intelligence*, 3(3):218–229, 2021.
- [19] J.-P. Noël and M. Schoukens. F-16 aircraft benchmark based on ground vibration test data. In *2017 Workshop on Nonlinear System Identification Benchmarks*, pages 19–23, 2017.
- [20] A. Norcliffe, C. Bodnar, B. Day, N. Simidjievski, and P. Liò. On Second Order Behaviour in Augmented Neural ODEs. *arXiv:2006.07220 [cs, stat]*, Oct. 2020.
- [21] A. Radford, K. Narasimhan, T. Salimans, and I. Sutskever. Improving language understanding by generative pre-training. 2018.
- [22] D. S.-S. Shieh, Y. Chang, and G. Carmichael. The evaluation of numerical techniques for solution of stiff ordinary differential equations arising from chemical kinetic problems. *Environmental Software*, 3(1):28–38, 1988.
- [23] M. Small. *Applied nonlinear time series analysis: applications in physics, physiology and finance*, volume 52. World Scientific, 2005.
- [24] E. Süli and D. F. Mayers. *An introduction to numerical analysis*. Cambridge university press, 2003.
- [25] M. Valtonen and H. Karttunen. *The three-body problem*. Cambridge University Press, 2006.
- [26] A. Vaswani, N. Shazeer, N. Parmar, J. Uszkoreit, L. Jones, A. N. Gomez, L. u. Kaiser, and I. Polosukhin. Attention is all you need. In I. Guyon, U. V. Luxburg, S. Bengio, H. Wallach, R. Fergus, S. Vishwanathan, and R. Garnett, editors, *Advances in Neural Information Processing Systems*, volume 30. Curran Associates, Inc., 2017. URL <https://proceedings.neurips.cc/paper/2017/file/3f5ee243547dee91fbd053c1c4a845aa-Paper.pdf>.
- [27] S. Wiewel, M. Becher, and N. Thuerey. Latent space physics: Towards learning the temporal evolution of fluid flow. In *Computer graphics forum*, volume 38, pages 71–82. Wiley Online Library, 2019.
- [28] K. Yanai and Y. Kawano. Food image recognition using deep convolutional network with pre-training and fine-tuning. In *2015 IEEE International Conference on Multimedia & Expo Workshops (ICMEW)*, pages 1–6. IEEE, 2015.
- [29] Z. Yang, Z. Dai, Y. Yang, J. Carbonell, R. Salakhutdinov, and Q. V. Le. Xlnet: Generalized autoregressive pretraining for language understanding. *arXiv preprint arXiv:1906.08237*, 2019.
- [30] Y. Zhang. Progress and challenges in protein structure prediction. *Current opinion in structural biology*, 18(3):342–348, 2008.
- [31] J. Zhuang, N. Dvornik, X. Li, S. Tatikonda, X. Papademetris, and J. Duncan. Adaptive checkpoint adjoint method for gradient estimation in neural ode. In *International Conference on Machine Learning*, pages 11639–11649. PMLR, 2020.

A Experimental Details

All experiments are performed with Python 3.6 and PyTorch 1.8.1. We use differentiable ODE solver³ implemented by Chen et al. [1], and we choose the adaptive step size solver Dopri5 by default. The neural differential operator is trained on a single NVIDIA Tesla P100 GPU, and other experiments are on a single CPU. RNODE in our baseline regularizes the derivatives directly to zero, i.e., the loss function is $\tilde{\mathcal{L}} = \mathcal{L}(\mathcal{X}', \mathcal{X}) + \lambda \cdot \|f_{\Theta}(\mathcal{X}, \mathcal{T})\|_2^2$.

A.1 Neural Differential Operator

We implement all NDOs in following experiments by a 2-hidden-layer bidirectional LSTM followed by an output layer. Each hidden layer of LSTM has 128 units, and the output layer is defined as a 3-layer fully connected network 128-64-32-1 with ReLU activation. The hyperparameters of library \mathcal{Z}_{lib} are all set to be $(P, Q, C) = (3, 50, 10)$. We randomly draw 10000 function samples from \mathcal{Z}_{lib} and discretize them by 100 uniform random times in interval $[0, 1]$ as our training data. For the training process, we use Adam optimizer with an initial learning rate of 0.003 and decayed by CosineAnnealingLR scheduler. The minibatch size is set to 64 and we train for 641 epochs (100000 iterations).

For the first-order NDO, we set the input sequence as $(\mathcal{X}, \mathcal{T}, \Delta\mathcal{T}) = \{(x_i, t_i, \Delta t_i)\}_{i=0}^N$, where $\Delta t_i = t_i - t_{i-1}$, and the corresponding labels as $\dot{\mathcal{X}}$. For the second-order NDO, we set the input sequence as $(\dot{\mathcal{X}}, \mathcal{X}, \mathcal{T}, \Delta\mathcal{T}) = \{(\dot{x}_i, x_i, t_i, \Delta t_i)\}_{i=0}^N$, where $\Delta t_i = t_i - t_{i-1}$, and the corresponding labels as $\ddot{\mathcal{X}}$.

For the airplane vibration dataset, due to the number of training time points is 1000, we cut them into 10 segments with 100 time points in each segment, to adapt to the above NDOs trained on 100 time points.

In the three-body problem, a position vector $\mathbf{r}(t)$ in 3-dimensional space can be written in the parametric form $\mathbf{r}(t) = (r_1(t), r_2(t), r_3(t))$. Thus, we define the input of the first-order NDO as $(\mathcal{X}_1, \mathcal{X}_2, \mathcal{X}_3, \mathcal{T}, \Delta\mathcal{T}) = \{(x_{1i}, x_{2i}, x_{3i}, t_i, \Delta t_i)\}_{i=0}^N$, where $\mathcal{X}_1, \mathcal{X}_2, \mathcal{X}_3$ can be generated from three independent function samples drawn from the library \mathcal{Z}_{lib} . The corresponding label is $(\dot{\mathcal{X}}_1, \dot{\mathcal{X}}_2, \dot{\mathcal{X}}_3)$. The second-order NDO can be similarly defined and trained for this task.

A.2 Experiments on Physical Systems

Planar Spiral Systems We train all models for 2000 iterations by Adam optimizer with an initial learning rate of 0.1 and decayed by a factor of 0.995 at each iteration. The state of the ODEs is defined as $[x, y]$, and we apply first-order NDO separately on the trajectories $(x_i)_{i=1}^N$ and $(y_i)_{i=1}^N$ to get corresponding estimated derivatives $(\dot{x}_i)_{i=1}^N$ and $(\dot{y}_i)_{i=1}^N$. For NDO-NODE and RNODE, we grid search the strength λ in range $[10^{-4}, 10]$ for the best performance. We choose $\lambda = 0.08, 0.08, 0.01, 0.005$ for NDO-NODE under noise scales $\sigma = 0, 0.01, 0.03, 0.05$, respectively, and $\lambda = 0.0001, 0.0001, 0.0001, 0.0001$ for RNODE. Figure 8 shows the training MSE loss of these models under different noise scales.

Damped Harmonic Oscillator Similar to the setting in Norcliffe et al. [20], we train all models for 2000 iterations by Adam optimizer with an initial learning rate of 0.01 and decayed by a factor of 0.999 at each iteration. Let $x, v = \frac{dx}{dt}$ and $a = \frac{dv}{dt}$ denotes the position, velocity and acceleration of the oscillator, respectively. We model the state of the ODEs as $[x, v]$. To get the corresponding estimated derivative $[v, a]$, we use first-order NDO to extract velocity estimations $(v_i)_{i=1}^N$ from position observations $(x_i)_{i=1}^N$, and then use second-order NDO to extract acceleration estimations $(a_i)_{i=1}^N$ from both observations $(x_i)_{i=1}^N$ and estimated velocities $(v_i)_{i=1}^N$. For $\sigma = 0, 0.1, 0.3, 0.5$, we choose $\lambda = 0.8, 0.02, 0.001, 0.001$ for NDO-NODE, and $\lambda = 0.001, 0.001, 0.01, 0.01$ for RNODE, after grid search λ in range $[10^{-4}, 10]$. Figure 9 shows the training MSE loss of these models under different noise scales.

³See their Github repo at <https://github.com/rtqichen/torchdiffeq>.

Three-body Problem Similar to the setting in Zhuang et al. [31], we train all models for 100 iterations by Adam optimizer with an initial learning rate of 0.1 and decayed by a factor of 0.995 at each iteration. Let \mathbf{r}_i , $\mathbf{v}_i = \frac{d\mathbf{r}_i}{dt}$, $\mathbf{a}_i = \frac{d\mathbf{v}_i}{dt}$, $i = 1, 2, 3$, denote the position, velocity and acceleration of i th body in 3-dimensional space, respectively. We model the state of ODEs as a 18-dimensional vector $[\mathbf{r}_1, \mathbf{r}_2, \mathbf{r}_3, \mathbf{v}_3, \mathbf{v}_3, \mathbf{v}_3]$. We use NDOs separately on each body to get the estimated derivatives, as mentioned in Section A.1. For the i th body, we use the first-order NDO on position observations $(\mathbf{r}_{ij})_{j=0}^N$ to get velocity estimations $(\mathbf{v}_{ij})_{j=0}^N$, and then use second-order NDO to estimate the acceleration $(\mathbf{a}_{ij})_{j=0}^N$ by positions and velocities. For $\sigma = 0, 0.001, 0.003, 0.005$, we choose $\lambda = 0.0008, 0.004, 0.0008, 0.0015$ for NDO-NODE, and $\lambda = 0.1, 0.007, 0.002, 0.004$ for RNODE, after grid search λ in range $[10^{-4}, 10]$. Figure 10 shows the training MSE loss of these models under different noise scales.

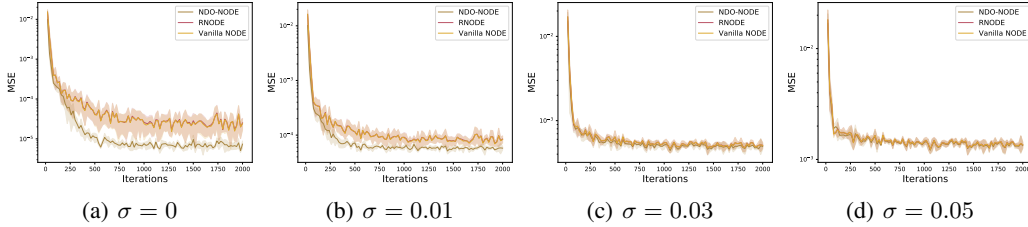


Figure 8: Training MSE loss of planar spiral systems under different noise scales.

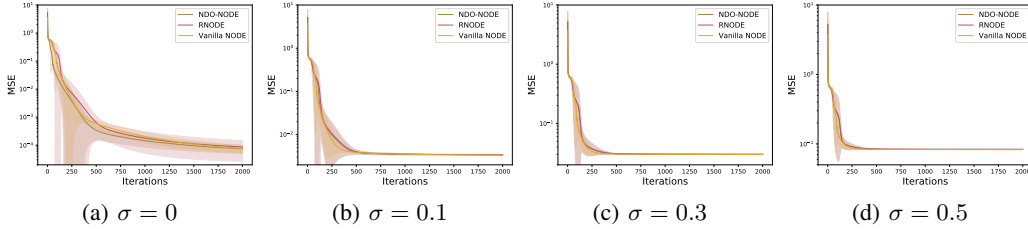


Figure 9: Training MSE loss of damped harmonic oscillator under different noise scales.

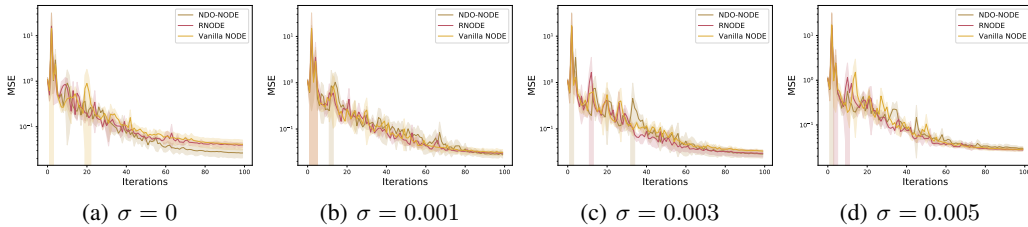


Figure 10: Training MSE loss of three-body problem under different noise scales.

A.3 Experiments on Stiff ODEs

Ghosh et al. [8] propose STEER that shows advantages in learning stiff ODEs, here we apply their experiment to test NDO-NODE. Following their setting, we train all models for 3000 iterations by RMSprop optimizer with learning rate 0.0001. The training dataset contains 120 points that equally sampled from time range $[0, 15]$. We model the state of ODEs as $[x]$, and we use first-order NDO to estimate the derivative $(\dot{x}_i)_{i=1}^N$ from observations $(x_i)_{i=1}^N$. For NDO-NODE and RNODE, we grid search λ in range $[10^{-4}, 10]$. For NDO-NODE, we set $\lambda = 0.05$. For RNODE, we set $\lambda = 0.001$. For NODE with STEER, it uses ODE solver implemented⁴ by Ghosh et al. [8] and the hyperparameter is set to be $b = 0.124$.

⁴See their Github repo at <https://github.com/arnabgho/steer>.

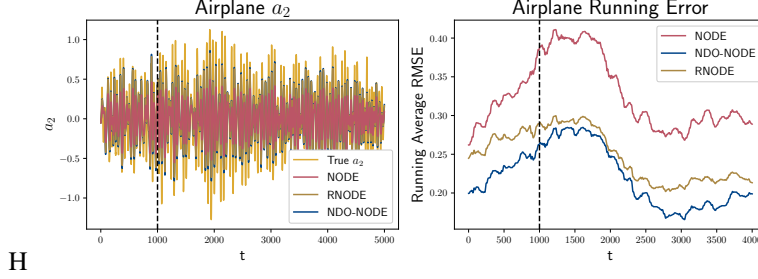


Figure 12: Results of vanilla NODE, NDO-SONODE and RNODE on airplane vibration dataset. **(Left)**: ground truth and forecasting trajectories. **(Right)**: moving averages of root mean square error (RMSE).

Additional Experiments on Another Stiff ODE Ghosh et al. [8] also test another stiff ODE

$$\frac{dy}{dt} = -1000y + 3000 - 2000e^{-t} + 1000\sin(t), \quad (10)$$

with initial condition $y(0) = 0$. This stiff ODE is much harder to learn as it does not become flat when time t gets larger. It is challenging for NODE to capture both the stiff and fluctuating parts. We train all models for 8000 iterations, as it is harder to learn. For NDO-NODE and RNODE, we grid search λ in range $[10^{-4}, 10]$. For NDO-NODE, we set $\lambda = 0.4$. For RNODE, we set $\lambda = 0.001$. We follow the same setting for STEER and other hyperparameters as [8]. The results is shown in Figure 11. We can observe that NDO-NODE does good on interpolation, although it is still hard to do extrapolation. However, other methods can not even fit the training set.

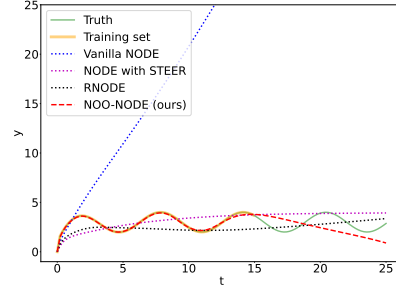


Figure 11: Results on the stiff ODE with sin term

A.4 Experiments on Airplane Vibration Dataset

As this task aims to learn nonlinear acceleration a_2 of the interface on the airplane, Norcliffe et al. [20] propose to use their method SONODE to try to capture the second-order information. In SONODE, the state of the underlying ODE is defined as $[a_2, z]$, where $z = \frac{da_2}{dt}$. Thus, we use both first-order NDO and second-order NDO to estimate the derivatives $[z, \dot{z}]$ and take this estimation as the enhanced signal in NDO-SONODE. We train these models for 1000 iterations by Adam optimizer with an initial learning rate of 0.01 and decayed by a factor of 0.995 at each iteration. For NDO-SONODE, we choose $\lambda = 0.1$.

Additional Experiments using first-order NODE As SONODE models this dataset as second-order ODE, we simplify this bias and model the state of the underlying ODE as $[a_2]$. We keep the networks, training, and test process unchanged, and evaluate the first-order NODE. For NDO-NODE, we set $\lambda = 0.005$. For RNODE, we set $\lambda = 0.0005$. The results is reported in Figure 12. From the results, we find this is hard to learn for vanilla first-order NODE without any bias or enhanced signals. However, with the help of the regularizer or NDO, the loss can get very close to SONODE.

B Proof for Theorem 3.1

Theorem B.1. Suppose that $\mathcal{Z}'_{lib} \subset \mathcal{Z}_{lib}$ is the training function set for NDO. The Lipschitz constant for the learned neural differential operator function is L_{NN} . For given continuous differentiable function $h(t) : [T_0, T_1] \rightarrow \mathbb{R}$, we define the distance between two functions as $\rho(h, z) = \sum_{i=1}^N |h(t_i) - z(t_i)|$, where $\{t_i\}_{i=1}^N$ equally partition the time interval $[T_0, T_1]$. $z(t) \in \mathcal{Z}'_{lib}$ is a function in the training data, $h(t)$ is an arbitrary function. The output derivative of NDO for a function is denoted using the subscription NDO. Then the error of the output derivation \dot{h}_{NDO} and the ground truth derivative \dot{h} can be upper bounded as:

$$\rho(\dot{h}_{NDO}, \dot{h}) \leq L_{NN} \int_{T_0}^{T_1} |z(t) - h(t)| dt + \int_{T_0}^{T_1} |\dot{z}(t) - \dot{h}(t)| dt + \frac{|T_1 - T_0|^3}{12N^2} M + \rho(\dot{z}_{NDO}, \dot{z}),$$

where $M = L_{NN} \cdot \max_{t \in [T_0, T_1]} |\ddot{\epsilon}(t)| + \max_{t \in [T_0, T_1]} |\dot{\epsilon}(t)|$ with $\epsilon(t) = |z(t) - h(t)|$.

Proof:

$$\begin{aligned}
\rho(\dot{h}_{\text{NDO}}, \dot{h}) &= \sum_{i=1}^N |\dot{h}_{\text{NDO}}(t_i) - \dot{h}(t_i)| \\
&= \sum_{i=1}^N |\dot{h}_{\text{NDO}}(t_i) - \dot{z}_{\text{NDO}}(t_i) + \dot{z}_{\text{NDO}}(t_i) - \dot{z}(t_i) + \dot{z}(t_i) - \dot{h}(t_i)| \\
&\leq \sum_{i=1}^N |\dot{h}_{\text{NDO}}(t_i) - \dot{z}_{\text{NDO}}(t_i)| + \sum_{i=1}^N |\dot{z}_{\text{NDO}}(t_i) - \dot{z}(t_i)| + \sum_{i=1}^N |\dot{z}(t_i) - \dot{h}(t_i)| \\
&\stackrel{(1)}{\leq} L_{\text{NN}} \cdot \sum_{i=1}^N |h(t_i) - z(t_i)| + \sum_{i=1}^N |\dot{z}_{\text{NDO}}(t_i) - \dot{z}(t_i)| + \sum_{i=1}^N |\dot{z}(t_i) - \dot{h}(t_i)| \\
&\stackrel{(2)}{\leq} \left(L_{\text{NN}} \int_{T_0}^{T_1} |h(t) - z(t)| dt + \frac{|T_1 - T_0|^3}{12N^2} \max_{t \in [T_0, T_1]} |\ddot{\epsilon}(t)| \right) \\
&\quad + \left(\int_{T_0}^{T_1} |\dot{h}(t) - \dot{z}(t)| dt + \frac{|T_1 - T_0|^3}{12N^2} \max_{t \in [T_0, T_1]} |\ddot{\epsilon}(t)| \right) + \rho(\dot{h}_{\text{NDO}}, \dot{h}),
\end{aligned}$$

where the inequality (1) is established according to the Lipschitz condition of the neural network⁵; the inequality (2) is established according to the numerical error between the integral and its discretization [24], i.e.,

$$\begin{aligned}
& \left| \sum_{i=1}^N |h(t_i) - z(t_i)| - \int_{T_0}^{T_1} |h(t) - z(t)| dt \right| \\
& \leq \sum_{i=1}^N \left| |h(t_i) - z(t_i)| - \int_{t_i}^{t_{i+1}} |h(t) - z(t)| dt \right| \\
& \stackrel{(3)}{\leq} N \cdot \frac{|T_1 - T_0|^3}{12N^2} \max_{t \in [T_0, T_1]} \ddot{\epsilon}(t) \\
& \leq \frac{|T_1 - T_0|^3}{12N^2} \max_{t \in [T_0, T_1]} \ddot{\epsilon}(t)
\end{aligned}$$

where the inequality (3) is established according to Theorem 7.1 in [24], and $\epsilon(t) = |h(t) - z(t)|$. Similarly, we have $\left| \sum_{i=1}^N |\dot{h}(t_i) - \dot{z}(t_i)| - \int_{T_0}^{T_1} |\dot{h}(t) - \dot{z}(t)| dt \right| \leq \frac{|T_1 - T_0|^3}{12N^2} \ddot{\epsilon}(t)$.

⁵"The Lipschitz constant for the learned neural differential operator function is L_{NN} " means that $\|\dot{h}_{\text{NDO}} - \dot{z}_{\text{NDO}}\| \leq L_{\text{NN}} \|h - z\|$, where $\|z\| = \frac{1}{N} \sum_{i=1}^N |z(t_i)|$.